

Article

Remediation of PO_4^{3-} in Water Using Biodegradable Materials Embedded with Lanthanum Oxide Nanoparticles

Kai Guo ^{*}, Zirui Song and Chengchun Tang ^{*}

Hebei Key Laboratory of Boron Nitride Micro and Nano Materials, School of Materials Science and Engineering, Hebei University of Technology, Tianjin 300130, China; szr19961019@163.com

^{*} Correspondence: kaiguo@hebut.edu.cn (K.G.); tangcc@hebut.edu.cn (C.T.)

Abstract: Eutrophication, a process in which algae grow inordinately, adversely affects aqueous fauna. Phosphorous at levels above 0.1 mg/L is adequate to cause eutrophication. In this study, we aimed to reduce the amount of PO_4^{3-} in water using biodegradable and ecofriendly sorbents. Lanthanum oxide nanoparticles were doped in agar and cellulose sponge to produce two new sorbents, *agar-La* and *sponge-La*, respectively. Both sorbents showed high efficacy in remediating up to 10 mg/L PO_4^{3-} in water. *Sponge-La* was found to be more proficient in terms of adsorption than *agar-La* because it required just 1 h to achieve 80% adsorption when the initial concentration of PO_4^{3-} was 10 mg/L. *Sponge-La* was effective at pH levels ranging from 4 to 8, with a removal rate of 80–100%. Although *agar-La* displayed a slow sorption process, it presented a high adsorption capacity (156 mg/g); moreover, the cake-shaped *agar-La* could be easily manufactured and separated from an aqueous matrix or any water-based solutions. These two sorbents could effectively remove high concentrations of PO_4^{3-} , and their preparation requires a simple step. *Agar-La* was easier to manufacture, whereas the adsorption process using *sponge-La* was more rapid. In addition, both sorbents can be easily separated from the matrix after sorption.

Keywords: lanthanum oxide nanoparticles; agar; sponge; PO_4^{3-} ; eutrophication; adsorption



Citation: Guo, K.; Song, Z.; Tang, C.

Remediation of PO_4^{3-} in Water

Using Biodegradable Materials

Embedded with Lanthanum Oxide

Nanoparticles. *Water* **2022**, *14*, 1656.

<https://doi.org/10.3390/w14101656>

Academic Editor: Constantinos

V. Chrysikopoulos

Received: 26 April 2022

Accepted: 20 May 2022

Published: 23 May 2022

Publisher's Note: MDPI stays neutral with regard to jurisdictional claims in published maps and institutional affiliations.



Copyright: © 2022 by the authors. Licensee MDPI, Basel, Switzerland. This article is an open access article distributed under the terms and conditions of the Creative Commons Attribution (CC BY) license (<https://creativecommons.org/licenses/by/4.0/>).

1. Introduction

Eutrophication, during which algae grow inordinately, is a global problem that threatens the survival of aqueous fauna due to hypoxia and toxins [1,2]. Some coastal areas, such as the Bohai Sea, China, are vulnerable to eutrophication owing to their relatively enclosed terrain [3]. Despite efforts for decades to manage nutrient loads in the Chesapeake Bay watershed, the water quality of the estuary area has not improved [4]. P is one of the primary factors causing eutrophication; P at levels above 0.1 mg/L is adequate for the occurrence of eutrophication [5]. The level of P has been higher than that of N in the Bohai Sea area over the last 40 years [6]. P is predominantly present as PO_4^{3-} in water because of its high solubility [7]. A large amount of PO_4^{3-} in water is chemically precipitated with Fe, Ca, and Al compounds [8,9]; however, the precipitated P is difficult to recycle. Liu and his coworkers applied an electrical field to intensify the migration of PO_4^{3-} to an Al/C electrode, which is derived from a metal-organic framework (MOF) [10]; however, the installation of this device is expensive.

The adsorption process has been used to effectively remove PO_4^{3-} from water. The ability of natural minerals, such as dolomite and hydroxyapatite, to adsorb PO_4^{3-} has been investigated [11]. Using structural modulation during calcination, CaFe-layered double hydroxides were synthesized to adsorb PO_4^{3-} [12]. To date, the most common strategy has been the use of a composite comprising a carrier with a high surface area, such as meso-silica [13], or with high encapsulation ability, such as MOFs [14,15], and with another compound with a high affinity to PO_4^{3-} . A magnetic MOF, $\text{Fe}_3\text{O}_4@\text{MIL-101}(\text{Cr})$, which is feasible for recycling, has been synthesized to adsorb arsenate and PO_4^{3-}

without interference [16]. Fe/Al(NO₃⁻) MOF shows a high PO₄³⁻-adsorption capacity but the introduction of N into the matrix aggravates eutrophication [17]. Sulfonic acid introduced into a Cu-based MOF shows high efficacy for PO₄³⁻ adsorption [18]. However, the complexity of the ligand increases the difficulty of synthesis. Zr(IV) has been embedded in biochar activated with chitosan–soya-bean husk for PO₄³⁻ adsorption [19]. As biochar is highly dispersive, a gel-like sorbent made of zirconium oxide and polystyrene offsets this limitation [20]. Moreover, some rare earth elements other than Zr that hardly coordinate with ligands, such as La and Ce, have a high affinity for PO₄³⁻, which is supported by the hard–soft acid–base theory; therefore, these metals have been intensively studied [21,22]. A Ce-doped MOF, UiO-66-NH₂, captured PO₄³⁻ intensively, and the input of amine-introduced N in the solution [23]. Min et al. [24] modified a UiO-66 MOF using La, which showed a phenomenal PO₄³⁻-adsorption capacity. However, the collection of La after each cycle of adsorption is not convenient. Although La-loaded biochar [25] and bentonite [26] are effective in removing PO₄³⁻, it is necessary to find a suitable carrier that is intact and unbreakable in harsh environments. Ribet et al. [27] imparted magnetite iron oxide (Fe₃O₄) to a cellulose sponge, which is cheap and biodegradable, to adsorb PO₄³⁻ proficiently. An La-loaded magnetic hydrogel has been reported to achieve 105.72 ± 5.99 mg P/g adsorption capacity [28]. The membrane was designed to modify the La–Zn(4,4-dipy)(OAc)₂/bacterial cellulose composite with tannic acid [29]. Al(OH)₃ nanocrystals have been grown in an *Artemia* Cyst shell to achieve a high PO₄³⁻-adsorption capacity [30].

In this study, we aim to reduce the amount of PO₄³⁻ in water using biodegradable and ecofriendly sorbents. We postulate that lanthanum oxide nanoparticles (LONP) combined with cellulose sponge (*sponge-La*) can adsorb PO₄³⁻ with high efficacy. Additionally, we designed an LONP-containing sorbent using agar as the carrier (*agar-La*). Agar is an ideal carrier because it is cheap and biodegradable, and its shape can be easily manipulated. The preparation of these two sorbents requires a simple step: assembling the two components, the LONP and the carrier. In addition, it is easy to separate the sorbent from the matrix after sorption; no complex filtration techniques are required. We aim to evaluate the detailed practical aspects of each sorbent and justify its application.

2. Materials and Methods

2.1. Reagents and Apparatus

Lanthanum (III) nitrate, sodium hydroxide, and potassium dihydrogen PO₄³⁻ were purchased from Tianjin Jinke Fine Chemicals Co., Ltd. (Tianjin, China). Agar was procured from Qingdao Hope Bio-Technology Co., Ltd. (Qingdao, China). Cellulose sponge was obtained from Scotch-Brite (3M Co., Shanghai, China).

A horizontal shaker (SHY-2 water-bath shaker, Dadi Auto-Instrumentation Co., Baoding, China) was applied for the adsorption experiment.

2.2. Instruments

Instruments used to characterize the materials were as follows: X-ray photoelectron spectroscopy (XPS) system (ESCALAB 250Xi; Thermo Fisher Scientific, Waltham, MA, USA), Fourier transform infrared spectroscopy (FTIR) system (TENSOR 27; Bruker, Germany), transmission electron microscopy (TEM) system (JEM 2100F; JEOL, Tokyo, Japan), scanning electron microscopy associated with energy dispersive spectroscopy (EDS) system (Apreo 2C; Thermo Fisher Scientific, San Jose, CA, USA), and X-ray diffraction (XRD) analysis system (D8 Discover; Bruker AXS, Karlsruhe, Germany). MI-100S Water Analysis Device (Massinno Co., Ltd., Tianjin, China) was used to determine the concentration of total P. Alternatively, a microplate reader (JC1086-A; Qingdao Juchuang Environmental Protection Co., Ltd., Qingdao, China) was used to determine P concentration.

2.3. Synthesis of LONPs

First, LONPs were synthesized using Fang's method [31]. In 40 mL of deionized water, 6 mmol La(NO₃)₃·6H₂O and 18 mmol NaOH were dissolved and stirred for 10 min. The

white precipitate produced was transferred to an 80 mL autoclave tube and heated for 12 h at 120 °C. The product was then washed with deionized water and centrifuged five times at $100,000 \times g$ for 10 min each time. The supernatant was decanted, and the precipitate (LONP) was freeze-dried overnight.

2.4. Preparation of Agar–La

To prepare the *agar–La* membrane, 390 mg of agar and 50 mg of La were added to 10 mL of deionized water and boiled. The boiled solution was immediately poured into a ring mold (diameter = 3.8 cm) on a glass plate. The hot fluid was cooled for 10 min and solidified as a malleable membrane (Supplementary Figure S1).

2.5. Preparation of Sponge–La

To prepare *sponge–La*, 0.10 g of LONP was added to 100 mL of deionized water and stirred at 35 °C. The cellulose sponge was immersed in the emulsion for 2 h. Thereafter, the cellulose sponge was dried at 60 °C in a box furnace for 1 h.

2.6. Analysis of Sponge–La

To examine the actual effect of the sponge sorbent in sewage, we added pure sponge and *sponge–La* to the sewer from a residential kitchen. Several parameters, including total P (TP), total N (TN), and $\text{NH}_4^+\text{-N}$, reflecting the water quality were measured using a water analysis device (MI-100S; Massinno Co., Ltd., Tianjin, China).

2.7. Analysis of PO_4^{3-}

PO_4^{3-} was analyzed using the ammonium molybdate spectrophotometric method [32]. This is a standardized method regulated by the Ministry of Ecology and Environment in China. The water quality testing device that we used was equipped with reagent kits for the analysis.

2.8. Adsorption and Desorption Study

For adsorption study, 10 mL phosphate-spiked solution and 0.1 g sorbent were added to a small glass vial with pH ~6, which was then placed into a horizontal shaker to agitate at 30 °C.

For desorption study, the phosphate-contained sorbent was added to 10-mL 0.1 M NaOH in the glass vial, which was then placed into the horizontal shaker to agitate at 25 °C.

Formula used are:

Adsorption capacity:

$$c = \frac{V(c_{ini} - c_{equ})}{m}$$

where V (L) is the volume of spiked solution; c_{ini} (mg/L) and c_{equ} (mg/L) are the initial and equilibrium concentration of phosphate, respectively; m (g) is the mass of sorbent.

Adsorption rate:

$$r = \frac{c_{ini} - c_{equ}}{c_{ini}} \times 100\%$$

3. Results and Discussion

3.1. Characterization

The XRD spectra of the *agar–La* membrane displayed sharper peaks in the crystalline structural features than the control (pure agar) because of La doping (Supplementary Figure S2a). In addition to the peaks of pure sponge, a sharper peak was observed for *sponge–La* owing to the crystalline form of La (Supplementary Figure S2b). When the *sponge–La* sorbent was added to actual sewage, the overall spectra shifted to the left, implying that the *sponge–La* could adsorb more fouling agents than pure sponge (Supplementary Figure S2c).

Because of the addition of LONP, sleeker lines were observed in the TEM image of *agar-La* (Supplementary Figure S3a,d) and *sponge-La* (Supplementary Figure S3f) than those of agar (Supplementary Figure S3b,e) and pure sponge (Supplementary Figure S3c). The rough surface of pure agar created spots for the binding of LONP. Moreover, the tendency to form a lamellar structure after doping LONP in the agar (Figure 1) was confirmed by EDS mapping, which showed that the La weight percent of *agar-La* was higher (Figure 1d) than that of pure agar (Figure 1c). The pure agar had a rugged structure, whereas *agar-La* displayed crystalline lines attributed to La, which was confirmed by EDS mapping, where the weight percent of La was 22.1% and that of P was 1.8% because of the adsorbed PO_4^{3-} (Figure 1e).

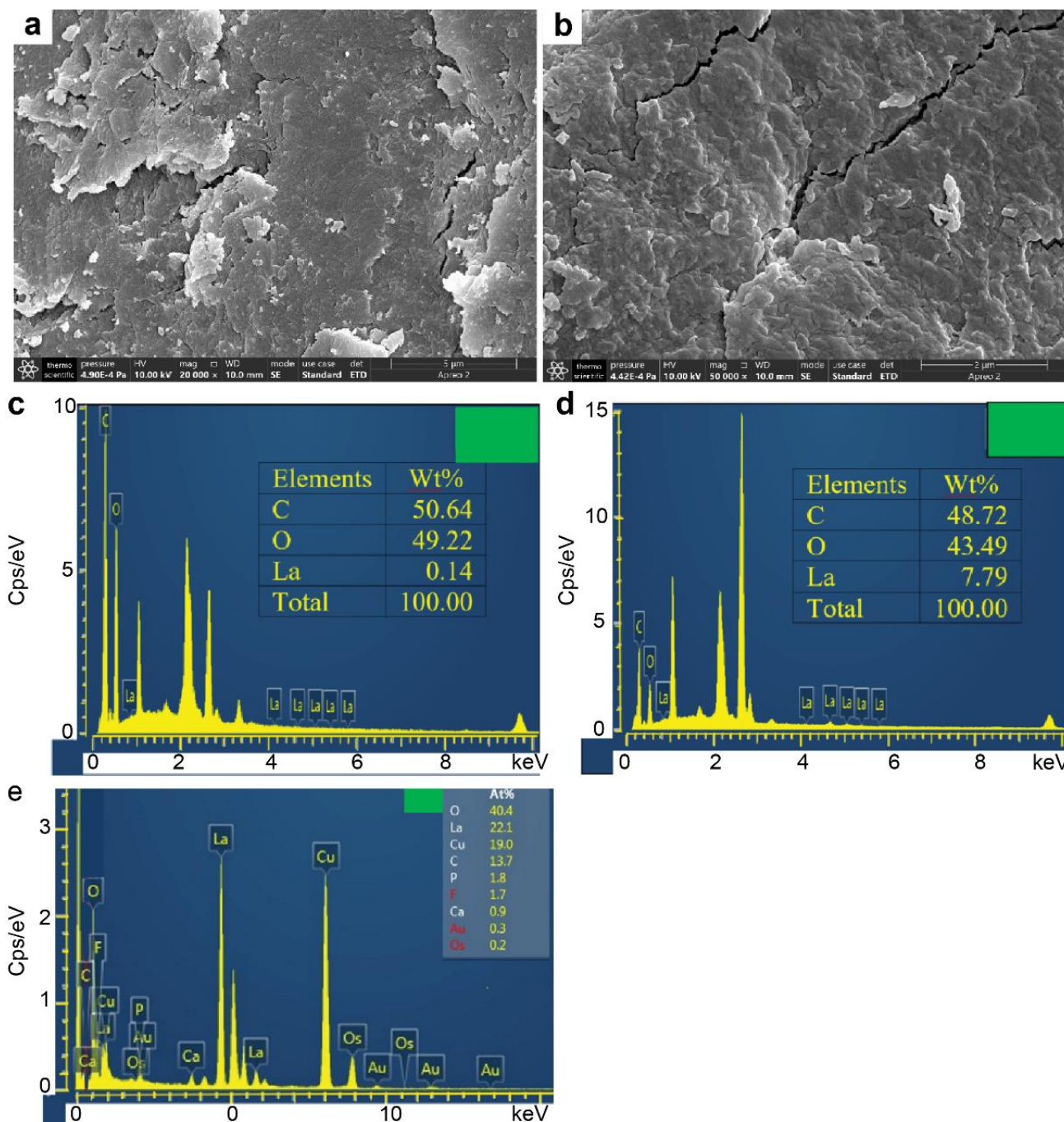


Figure 1. Scanning electron microscopy (SEM) images of agar (a) and *agar-La* (b); energy-dispersive spectroscopy (EDS) mapping of pure agar (c), *agar-La* (d), and *agar-La- PO_4^{3-}* (e).

The honeycombed multiporous structure of sponge (Figure 2a,b) and *sponge-La* (Figure 2c,d) are observed. Meanwhile, the loaded La are distinctive for *sponge-La*, which can be confirmed from EDS analysis (Figure 2f), which presents 1.67 wt% La.

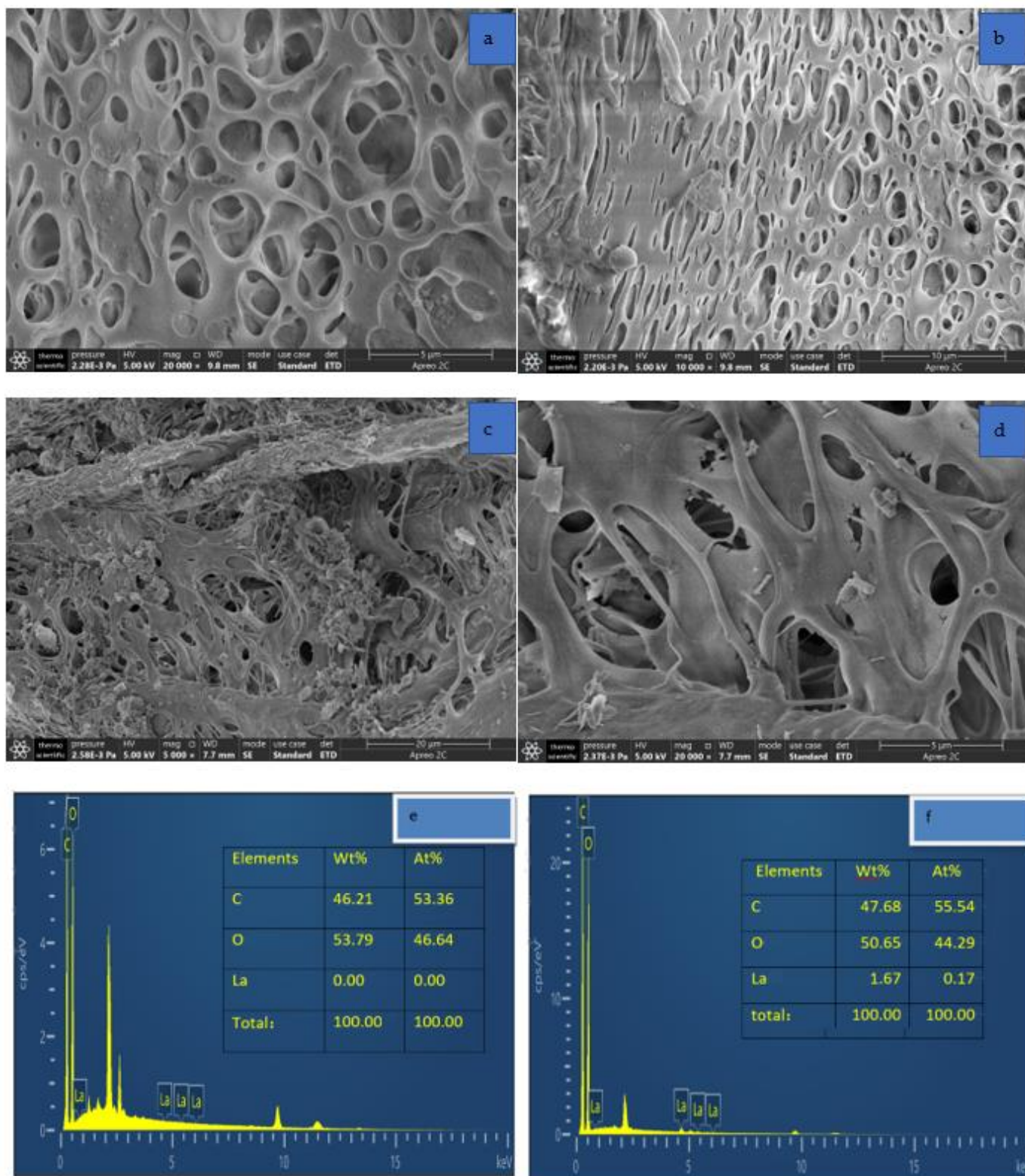


Figure 2. SEM images of sponge (a,b) and *sponge-La* (c,d), and EDS analysis of sponge (e) and *sponge-La* (f).

Two *agar-La* samples, pH6-A and pH6-B (replicates under pH 6) showed adsorption at pH 6. After the sorption process, pure agar, *agar-La*, and the two *agar-La* samples were characterized using FTIR (Supplementary Figure S4a). The intensity of the broad peak representing hydrogen bonds associated with hydroxyl groups at approximately 3450 cm^{-1} gradually weakened. This weakening occurred the fastest in agar, followed by *agar-La*, pH6-A, and pH6-B, because of the adsorbed La and P.

The carboxyl groups (at approximately 1650 cm^{-1}) evolved in a similar pattern, indicating that the adsorbed PO_4^{3-} chemically disrupted the original structure of agar. The peak at 1410 cm^{-1} , belonging to agar, gradually split into two peaks at 1450 and 1376 cm^{-1} after the adsorption of P on *agar-La*. As a result, the peak at 1450 cm^{-1} appeared only for pH6-A and pH6-B.

To compare the difference between FTIR spectra of sponge and *sponge-La* (Supplementary Figure S4b), the moderately weak peak under $\sim 1400\text{ cm}^{-1}$ (carboxylic acid group) is flattened for *sponge-La*, indicating the chemical modification between sponge and La^{3+} .

The XPS spectra of *agar-La* sorbents at initial PO_4^{3-} concentrations 5 and 10 mg/L (Supplementary Figure S5) demonstrated the difference between the following two adsorption scenarios: the different initial concentrations (5 and 10 mg/L) of PO_4^{3-} and the new bond formed at 830.1 eV when the initial concentration was 10 mg/L. The results imply that in the matrix containing a higher concentration of PO_4^{3-} , La^{3+} had a higher probability of forming a chemical bond with PO_4^{3-} .

3.2. Adsorption Study

Figure 3 illustrates the adsorption performance of the membranes when the initial concentration of total P is different. The actual initial concentration of total P was measured at 10 h. on the first day. After the measurement, all tubes were placed in a horizontal shaker and incubated at $30\text{ }^\circ\text{C}$. The next day, each sample was collected at 9 h (23 h after) to determine the P concentration, and the results are denoted as A on the x-axis. The samples were tested again at 15 h (29 h after) on the same day, and the results are denoted as B on the x-axis. On day 3, the samples were tested at 9 h (35 h after), and the results are denoted as C on the same axis. To analyze the adsorption capacity, Figure 3b shows that as initial concentration of phosphate elevates to 20 mg/L, the saturation of adsorption starts to surface. When it comes to 50 mg/L, the maximum adsorption capacity is stabilized to 150 mg/g.

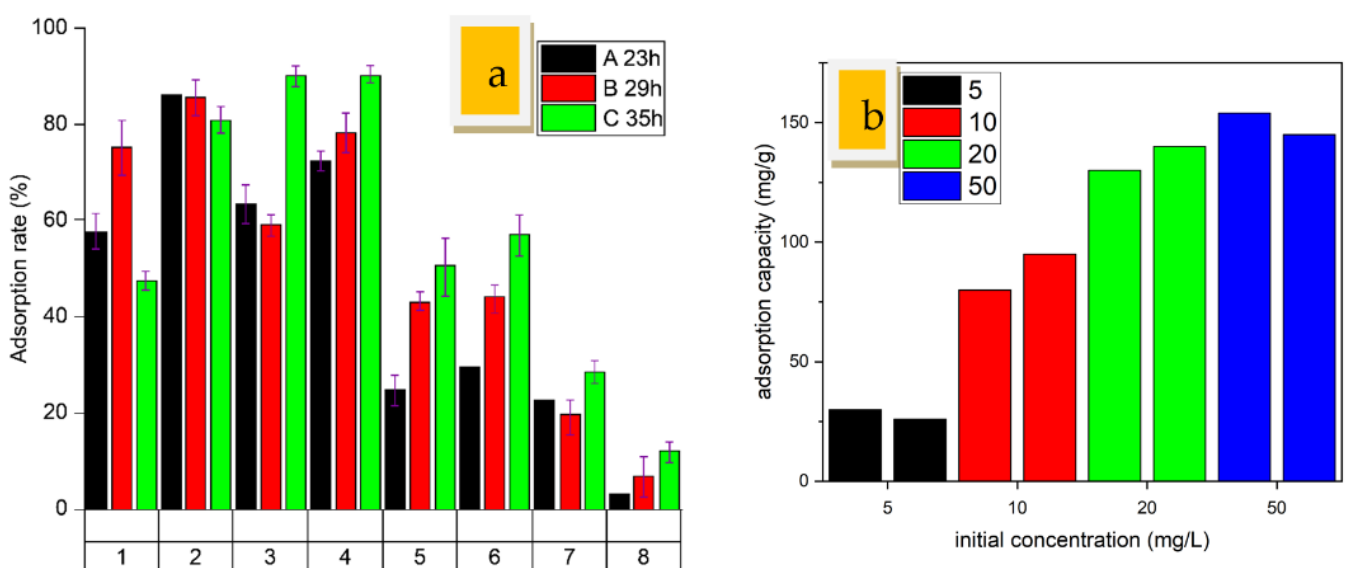


Figure 3. Adsorption rate (a) and capacity (b) by *agar-La* under different initial concentrations of phosphorous. The numbers 1 to 8 on the x-axis represent 5, 5, 10, 10, 20, 20, 50, and 50 mg/L, respectively.

For Columns 1 and 2, denoting 5 mg/L initial concentration on the second day of adsorption, the maximum adsorption capacity, approximately 80% removal rate, was achieved. Subsequently, the adsorption started to recede. However, when the initial concentration started to increase on day 3, the removal rate was higher than that on the previous day. The highest removal rate, approximately 90%, was observed at an initial concentration of 10 mg/L. As shown in Supplementary Figure S5, a new bond occurred in the La 3D spectra at this initial concentration, and it might be related to the chemical bonding between La^{3+} and PO_4^{3-} . The highest removal rate declined to 10% at an initial concentration of 50 mg/L.

To determine the best-fit isotherm curve, all adsorption scenarios for *agar-La* were plotted (Supplementary Figure S6a). The maximum adsorption capacity was approximately 150 mg/g, which was observed when the equilibrium concentration of PO_4^{3-} was higher than 15 mg/L. The Langmuir curve ($R^2 = 0.82$) fit the adsorption more adaptably than the Freundlich curve ($R^2 = 0.81$). However, the curves were also similarly overlapped, indicating the co-existence of monolayer and multilayer adsorption.

Cellulose sponges completed the sorption process faster than agar membranes (Figure 4). The initial concentration of PO_4^{3-} used was 10 mg/L. For all solutions, the PO_4^{3-} concentration was tested 1 h after adsorption. The PO_4^{3-} removal rate was 30% when only the pure sponge was used, and the *sponge-La* significantly improved this to above 80%. The maximum removal rate was achieved in both control (40%) and *sponge-La* groups (100%) 3 h after adsorption. This was favorable, and it indicates the scope of field studies for PO_4^{3-} removal in the future. After 4 h, the PO_4^{3-} removal rate of *sponge-La* remained 100% but that of the sponge started to recede thereafter, as indicated by its poor PO_4^{3-} content (Supplementary Figure S7). The adsorption capacity quickly approached to the maximum, after only 1 h of the adsorption process (Figure 4b). Subsequently, in the isotherm study, the adsorption capacity levels up at 20 mg/L; of which the maximum value approaches to 160 mg/g. The simulation shows that Langmuir is the best-fit (Supplementary Figure S6b), indicating the monolayer chemisorption process. Besides, the adsorption rate is high at low concentration but declines when it is above 20 mg/L (Figure 4c). Additionally, pseudo-first and second-order models were attempted for simulation. Pseudo-first-order ($R^2 = 0.92$) indicates the rapid adsorption process for *sponge-La*, while pseudo-second-order ($R^2 = 0.996$) is attributed to chemisorption process (Figure 4d). Overall, *sponge-La* proved to be more effective and efficient than pure sponges in removing excess PO_4^{3-} from water.

When *agar-La* was used, pH had a profound effect on adsorption. Samples of different pH levels were prepared by adding 0.1 M HCl (aq.) and 0.1 M NaOH dropwise to 10 mg/L PO_4^{3-} solution. The samples were collected after 16 h of adsorption, and pH was measured to determine data fluctuations (Figure 5a). The pH showed an increasing trend, and the actual pH was skewed from the initial pH. When the initial pH was 4, it shifted to approximately 6. When the initial pH was 8, it shifted to a slightly lower pH and when the initial pH was 10, it transitioned to 9. This fluctuation can be attributed to the acidic factor of the reagent used (KH_2PO_4). When the removal rate was the highest, above 60%, the optimal pH was 6. After continuing for another 24 h, the removal rate reached approximately 90% (Figure 5b). The overall curve was bell-shaped, indicating poor sorption at either very low or very high pH. Moreover, the dark blue color of the water indicates a high concentration of PO_4^{3-} (Supplementary Figure S8).

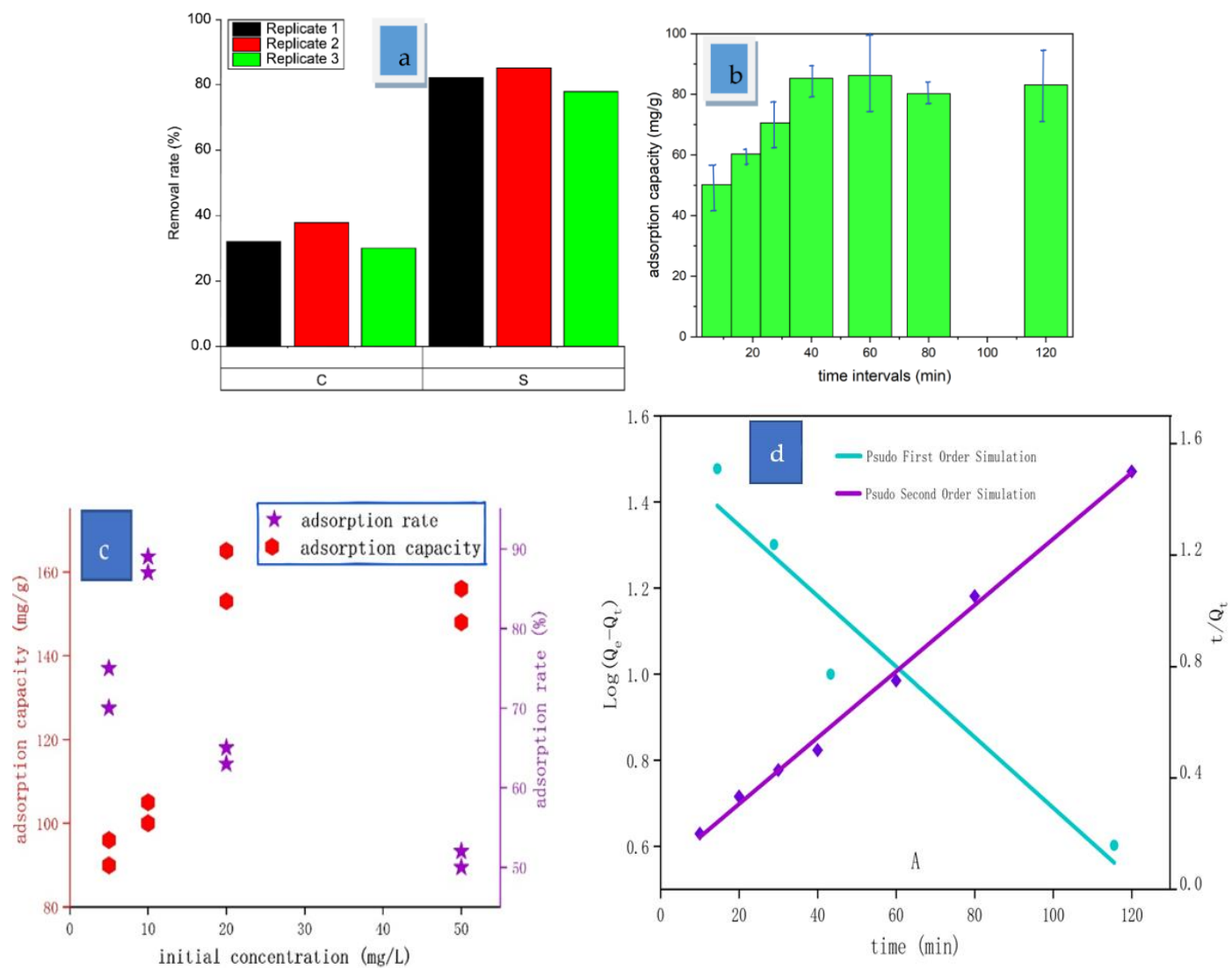


Figure 4. Comparison of adsorption completion after 1 h between sponge only (C) and *sponge-La* (S) (three replicates each) (a); adsorption capacity vs. time intervals for *sponge-La* (b); adsorption capacity and rate vs. initial concentration of phosphate for *sponge-La* (c); kinetic study of *sponge-La* (d).

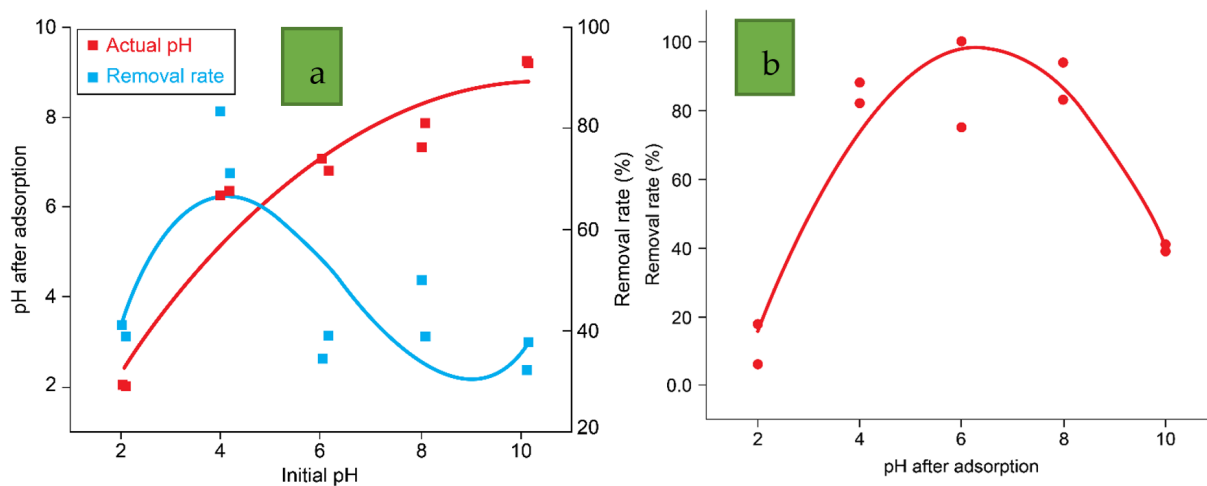


Figure 5. Effect of pH on the matrix of *agar-La* when the initial concentration of PO_4^{3-} was 10 mg/L (a); effect of pH on adsorption by *agar-La* after 40 h (b).

The analyses showed promising results, particularly for total N, which decreased to 0 mg/L after the application of *sponge-La* (Figure 6). The adsorption method was identical to that used in PO_4^{3-} adsorption. Although the sorbent was designed to ameliorate substantial amounts of total P, it was found to be effective for several other substances related to eutrophication. Nitrate input can indirectly affect PO_4^{3-} leaching to groundwater-fed wetlands because nitrate can directly lead to the mobilization of sulfate and immobilization of ferrous iron [33]. The relationship between N and P becomes the driving force for the selective adsorption of N rather than P when *sponge-La* is used in domestic sewage. Further research is required to ensure the selectivity and efficacy of P and N removal in an aqueous environment.

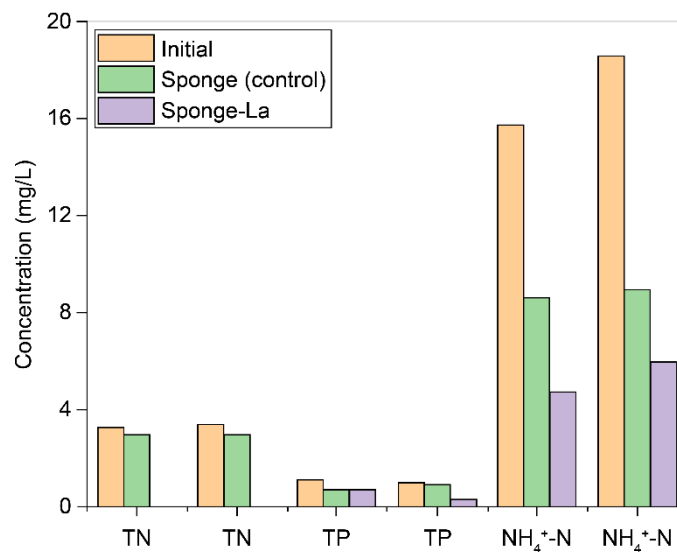


Figure 6. Several sewage analysis parameters showed a reduction in the concentration of major pollutants by *sponge-La*.

As for the desorption process (Figure 7a), after 3 h, majority phosphate is effectively released, when the original concentration is 10 mg/L, which brings potential to recycle phosphate after highly phosphate-polluted water is remediated using *sponge-La*. Furthermore, this sponge sorbent can maintain its ability after 4, 5 cycles (Figure 7b).

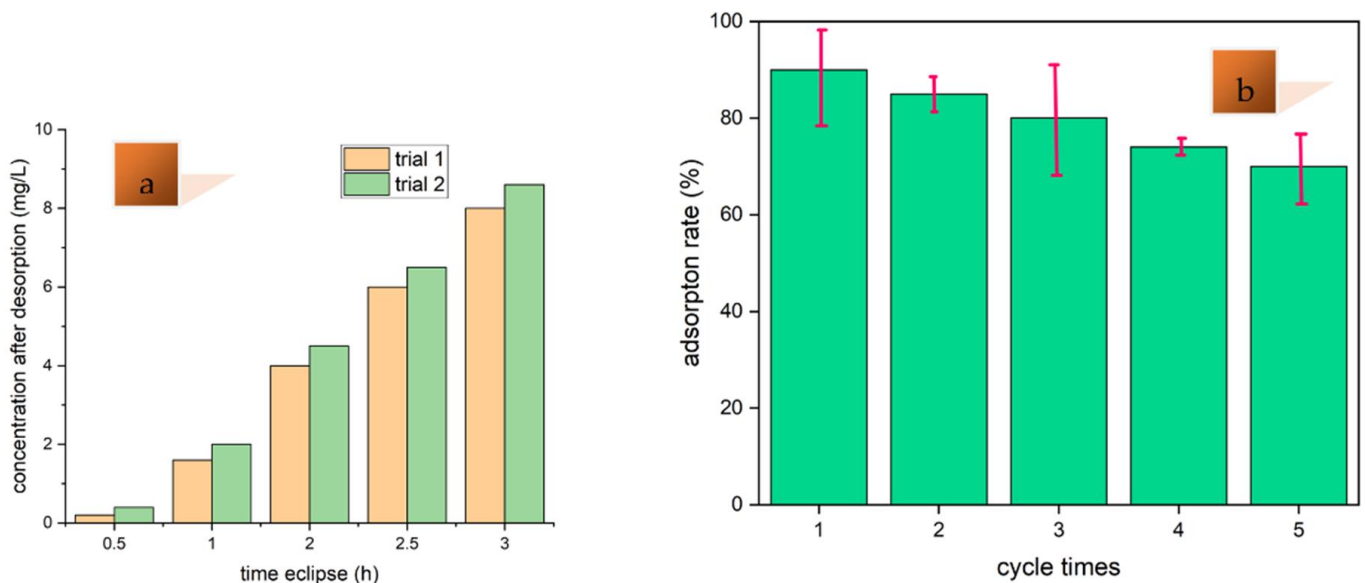


Figure 7. Desorption (a) and regeneration (b) study of *sponge-La*.

As shown in Table 1, our approach shows high potential to alleviate eutrophication compared to other sorbents, as *agar-La* has a high adsorption capacity, involves a simple synthesis method, and can separate from an aqueous matrix or water-based solutions. In addition, *sponge-La* can rapidly complete PO_4^{3-} adsorption.

Table 1. Comparison of other sorbents.

Type	Maximum Adsorption Capacity (mg/g)	Advantages	Disadvantages
La-MOF [24]	348.43	High adsorption capacity	Difficult to separate from solutions
Sulfonic acid-derived Cu-MOF [18]		High affinity to perchlorate and PO_4^{3-}	Difficult to synthesize
Ce-MOF [23]	211.86	High adsorption capacity	Introduction of N
Fe/Al(NO_3^-) MOF [17]	130	Selectivity to PO_4^{3-}	Introduction of N
La-modified bentonite [28]		Applicable to real aqua, and inexpensive	Difficult to separate from solutions
La biochar [25]	46.37	Applicable to real aqua	Low adsorption capacity, and difficult to separate from solutions
<i>Agar-La</i> (this study)	156	High adsorption capacity, easily separable from solutions, and simple synthesis	
<i>Sponge-La</i> (this study)	160	Rapid sorption process, applicable to actual sewers, which contain N	

3.3. PO_4^{3-} Analysis

During the ammonium molybdate method, the reaction between orthophosphate and ammonium molybdate occurs to form phosphorous-molybdenum hybrid acid, which is immediately reduced by ascorbic acid to produce a blue chelate. The darker the blue color, the higher the concentration of PO_4^{3-} in the water. This was observed when the sponge sorbent was used to remove 10 mg/L PO_4^{3-} in water. Supplementary Figure S9 represents the color distinction for samples with *sponge-La* (the first three replicates) and pure sponges (the last three replicates). A clear solution indicates that the majority of the PO_4^{3-} was absorbed by *sponge-La*.

However, this method required large quantities of reagents to complete the reaction, as each sample should be at least 5 mL, to which 0.2 mL of ammonium molybdate and 0.4 mL of ascorbic acid had to be added. Consequently, large quantities of reagents were wasted, which impeded the routine testing of PO_4^{3-} . Herein, we propose a rapid testing method that requires only a small number of samples and the reagents. In a 96-well transparent plate, 100 μL of sample was added, to which 10 μL of ammonium molybdate and 20 μL of ascorbic acid were added. Horizontally, the plate was gently shaken a few times, and the reaction was allowed to continue for 20 min. The plate was then placed in a microplate reader to measure the absorbance at 630 nm. The higher the absorbance, the higher the concentration of PO_4^{3-} . After 3 h of adsorption, the absorbance was several times higher for the pure sponge than for *sponge-La* (Figure 8a). The absorbance for *sponge-La* was 0.1 throughout, which inversely correlated to the removal rate tested—the lower the absorbance, the higher the removal rate. The relationship was examined in the pH study as well (Figure 8b). The lowest absorbance appeared at an initial pH of 4 (actual pH was 6), which corresponded to the highest removal rate. The highest absorbance was observed at extremely low and high pH levels.

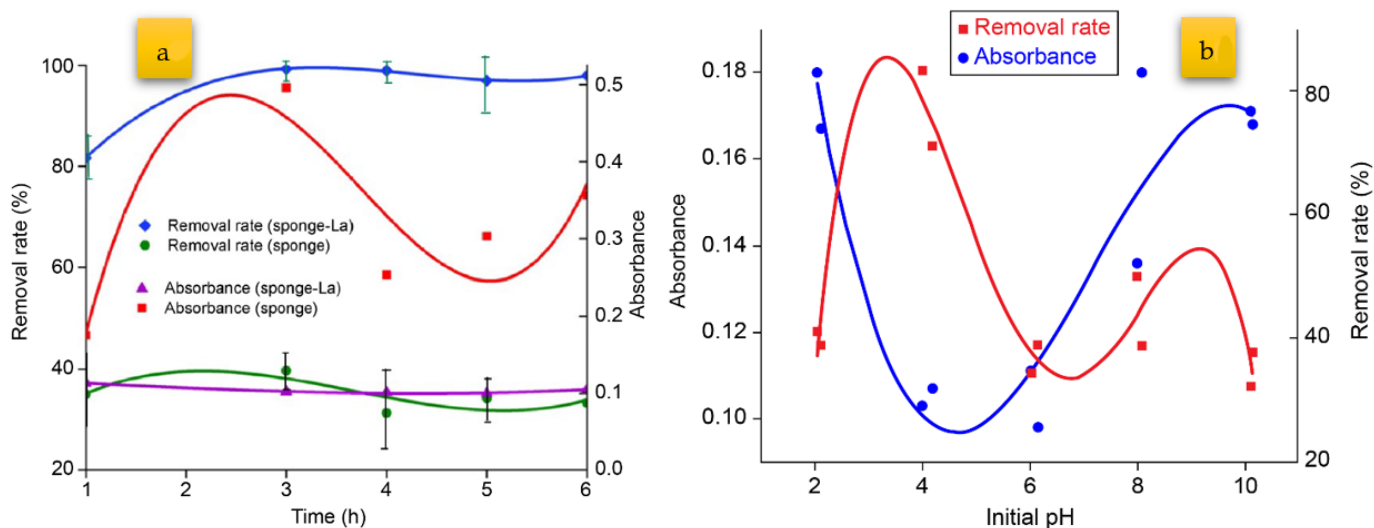


Figure 8. Inversely proportional relationship between absorbance and removal rate for *sponge-La* against different time intervals (a) and different pH (b).

To further confirm the effectiveness of the proposed adsorbents and determine any interference of other ions present in water, common competing ions for PO_4^{3-} in water, such as F^- and Na^+ , should be considered in future studies.

4. Conclusions

We designed two biodegradable and ecofriendly sorbents, *agar-La* and *sponge-La*, and demonstrated through removal experiments that they have promising applications in aqueous environments containing high PO_4^{3-} levels. *Agar-La* is cheaper and has a more modifiable shape than *sponge-La*; however, it requires a longer time to achieve adequate removal of PO_4^{3-} ions. In contrast, even though the raw material (sponge) for *Sponge-La* is expensive to procure, this sorbent can complete the sorption process rapidly. Both sorbents can acquire the maximum adsorption capacity around 150~160 mg/g. Furthermore, *agar-La* is stable in a wide pH range from 4–8, within which it maintains a high adsorption rate around 80~90%. Thus, an informed decision should be made when applying the two sorbents.

Supplementary Materials: The following supporting information can be downloaded at: <https://www.mdpi.com/article/10.3390/w14101656/s1>, Figure S1: Photograph of the prepared *agar-La* membrane showing its sheer and shiny appearance; Figure S2: X-ray diffraction (XRD) spectra of *agar-La* (a), *sponge-La* (b), and *sponge-La* in sewage treatment (c) compared with the controls; Figure S3: Transmission electron microscopy (TEM) images of *agar-La* (a,d), pure agar (b,e), sponge (c), and *sponge-La* (f); Figure S4: Fourier transfer infrared spectroscopy (FTIR) spectra of agar, *agar-La*, pH6-A, and pH6-B; Figure S5: X-ray photoelectron spectroscopy (XPS) images of La spectra at initial concentrations of 5 mg/L (a) and 10 mg/L (b); Figure S6: Adsorption isotherms of *agar-La*; Figure S7: Removal rate of control (C) and *sponge-La* sample (S) at different time intervals (black: 1 h; red: 3 h; and green: 4 h) from the start of the adsorption process; Figure S8: Color distinction among the water samples at different pH levels when using *agar-La* as the sorbent; Figure S9: Color differentiation after 1 h of adsorption using the ammonium-molybdate method. The clear initial three samples with *sponge-La* indicate the rapid sorption process.

Author Contributions: Conceptualization, K.G.; methodology, K.G.; software, K.G.; validation, K.G.; formal analysis, K.G.; investigation, K.G. and Z.S.; resources, K.G.; data curation, K.G. and Z.S.; writing—original draft preparation, K.G.; writing—review and editing, K.G.; visualization, K.G.; supervision, K.G. and C.T.; project administration, C.T.; funding acquisition, K.G. All authors have read and agreed to the published version of the manuscript.

Funding: This work was funded by the Tianjin Higher Education Collaboration Fund, grant number 280000364.

Data Availability Statement: Not applicable.

Acknowledgments: We appreciate instrumentation support including XRD, FTIR, XPS, and TEM from the Analysis Center for Advanced Materials, Hebei University of Technology; SEM support from Ceshigo Research Service (<https://www.ceshigo.com/> (accessed on 20 May 2022)). We appreciate laboratory assistance from graduate students, Gaoxing Wang, Jiaxiao Qiao, and Huayi Cai.

Conflicts of Interest: The authors declare no conflict of interest. The funders had no role in the design of the study; in the collection, analyses, or interpretation of data; in the writing of the manuscript, or in the decision to publish the results.

Abbreviations

LONP—lanthanum oxide nanoparticles; *sponge-La*—lanthanum oxide nanoparticles combined with cellulose sponge; *agar-La*—lanthanum oxide nanoparticles combined with agar.

References

1. Paul, B.; Bhattacharya, S.S.; Gogoi, N. Primacy of Ecological Engineering Tools for Combating Eutrophication: An Ecohydrological Assessment Pathway. *Sci. Total Environ.* **2021**, *762*, 143171. [[CrossRef](#)]
2. de Raús Maure, E.; Terauchi, G.; Ishizaka, J.; Clinton, N.; DeWitt, M. Globally Consistent Assessment of Coastal Eutrophication. *Nat. Commun.* **2021**, *12*, 6142. [[CrossRef](#)]
3. Xin, M.; Wang, B.; Xie, L.; Sun, X.; Wei, Q.; Liang, S.; Chen, K. Long-Term Changes in Nutrient Regimes and Their Ecological Effects in the Bohai Sea, China. *Mar. Pollut. Bull.* **2019**, *146*, 562–573. [[CrossRef](#)]
4. Murphy, R.R.; Keisman, J.; Harcum, J.; Karrh, R.R.; Lane, M.; Perry, E.S.; Zhang, Q. Nutrient Improvements in Chesapeake Bay: Direct Effect of Load Reductions and Implications for Coastal Management. *Environ. Sci. Technol.* **2022**, *56*, 260–270. [[CrossRef](#)]
5. Kumar, P.S.; Korving, L.; van Loosdrecht, M.C.M.; Witkamp, G.J. Adsorption as a Technology to Achieve Ultra-Low Concentrations of Phosphate: Research Gaps and Economic Analysis. *Water Res. X* **2019**, *4*, 100029. [[CrossRef](#)]
6. Wang, J.; Yu, Z.; Wei, Q.; Yao, Q. Long-Term Nutrient Variations in the Bohai Sea Over the Past 40 Years. *J. Geophys. Res. Ocean.* **2019**, *124*, 703–722. [[CrossRef](#)]
7. Water Resources—Nutrients and Eutrophication. Available online: <https://www.usgs.gov/mission-areas/water-resources/science/nutrients-and-eutrophication> (accessed on 22 December 2021).
8. Strom, P.F. *Technologies to Remove Phosphorus from Wastewater*; Rutgers University: New Brunswick, NJ, USA, 2006.
9. Zhang, Y.; Luo, P.; Zhao, S.; Kang, S.; Wang, P.; Zhou, M.; Lyu, J. Control and Remediation Methods for Eutrophic Lakes in the Past 30 Years. *Water Sci. Technol.* **2020**, *81*, 1099–1113. [[CrossRef](#)]
10. Liu, R.; Chi, L.; Feng, J.; Wang, X. MOFs-Derived Conductive Structure for High-Performance Removal/Release of Phosphate as Electrode Material. *Water Res.* **2020**, *184*, 116198. [[CrossRef](#)]
11. Boeykens, S.P.; Piol, M.N.; Samudio Legal, L.; Saralegui, A.B.; Vázquez, C. Eutrophication Decrease: Phosphate Adsorption Processes in Presence of Nitrates. *J. Environ. Manag.* **2017**, *203*, 888–895. [[CrossRef](#)]
12. Park, J.Y.; Lee, J.; Go, G.M.; Jang, B.; Cho, H.B.; Choa, Y.H. Removal Performance and Mechanism of Anti-Eutrophication Anions of Phosphate by CaFe Layered Double Hydroxides. *Appl. Surf. Sci.* **2021**, *548*, 149157. [[CrossRef](#)]
13. Awual, M.R. Efficient Phosphate Removal from Water for Controlling Eutrophication Using Novel Composite Adsorbent. *J. Clean. Prod.* **2019**, *228*, 1311–1319. [[CrossRef](#)]
14. Xie, Q.; Li, Y.; Lv, Z.; Zhou, H.; Yang, X.; Chen, J.; Guo, H. Effective Adsorption and Removal of Phosphate from Aqueous Solutions and Eutrophic Water by Fe-Based MOFs of MIL-101. *Sci. Rep.* **2017**, *7*, 3316. [[CrossRef](#)] [[PubMed](#)]
15. Huang, X.; Huang, L.; Babu Arulmani, S.R.; Yan, J.; Li, Q.; Tang, J.; Wan, K.; Zhang, H.; Xiao, T.; Shao, M. Research Progress of Metal Organic Frameworks and Their Derivatives for Adsorption of Anions in Water: A Review. *Environ. Res.* **2022**, *204*, 112381. [[CrossRef](#)] [[PubMed](#)]
16. Folens, K.; Leus, K.; Nicomel, N.R.; Meledina, M.; Turner, S.; Van Tendeloo, G.; Du Laing, G.; Van Der Voort, P. Fe₃O₄@MIL-101—A Selective and Regenerable Adsorbent for the Removal of As Species from Water. *Eur. J. Inorg. Chem.* **2016**, *2016*, 4395–4401. [[CrossRef](#)]
17. Li, S.; Liu, M.; Yin, C.; Chen, J.; Yang, X.; Wang, S. Tuning the Structure Flexibility of Metal-Organic Frameworks via Adjusting Precursor Anionic Species for Selective Removal of Phosphorus. *Process Saf. Environ. Prot.* **2020**, *143*, 322–331. [[CrossRef](#)]
18. Zhang, H.; Li, T.; Yang, Z.; Su, M.; Hou, L.; Chen, D.; Luo, D. Highly Efficient Removal of Perchlorate and Phosphate by Tailored Cationic Metal-Organic Frameworks Based on Sulfonic Ligand Linking with Cu-4,4'-Bipyridyl Chains. *Sep. Purif. Technol.* **2017**, *188*, 293–302. [[CrossRef](#)]

19. Banu, H.T.; Karthikeyan, P.; Meenakshi, S. Zr^{4+} Ions Embedded Chitosan-Soya Bean Husk Activated Bio-Char Composite Beads for the Recovery of Nitrate and Phosphate Ions from Aqueous Solution. *Int. J. Biol. Macromol.* **2019**, *130*, 573–583. [[CrossRef](#)]
20. Zhao, X.; Zhang, Y.; Pan, S.; Zhang, X.; Zhang, W.; Pan, B. Utilization of Gel-Type Polystyrene Host for Immobilization of Nano-Sized Hydrated Zirconium Oxides: A New Strategy for Enhanced Phosphate Removal. *Chemosphere* **2021**, *263*. [[CrossRef](#)]
21. Koh, K.Y.; Yang, Y.; Chen, J.P. Critical Review on Lanthanum-Based Materials Used for Water Purification through Adsorption of Inorganic Contaminants. *Crit. Rev. Environ. Sci. Technol.* **2022**, *52*, 1773–1823. [[CrossRef](#)]
22. Pearson, R.G. Hard and Soft Acids and Bases—The Evolution of a Chemical Concept. *Coord. Chem. Rev.* **1990**, *100*, 403–425. [[CrossRef](#)]
23. Liu, M.; Li, S.; Tang, N.; Wang, Y.; Yang, X.; Wang, S. Highly Efficient Capture of Phosphate from Water via Cerium-Doped Metal-Organic Frameworks. *J. Clean. Prod.* **2020**, *265*, 121782. [[CrossRef](#)]
24. Min, X.; Wu, X.; Shao, P.; Ren, Z.; Ding, L.; Luo, X. Ultra-High Capacity of Lanthanum-Doped UiO-66 for Phosphate Capture: Unusual Doping of Lanthanum by the Reduction of Coordination Number. *Chem. Eng. J.* **2019**, *358*, 321–330. [[CrossRef](#)]
25. Wang, Z.; Shen, D.; Shen, F.; Li, T. Phosphate Adsorption on Lanthanum Loaded Biochar. *Chemosphere* **2016**, *150*, 1–7. [[CrossRef](#)] [[PubMed](#)]
26. Zhou, Z.; Lin, C.; Li, S.; Liu, S.; Li, F.; Yuan, B. Four Kinds of Capping Materials for Controlling Phosphorus and Nitrogen Release from Contaminated Sediment Using a Static Simulation Experiment. *Front. Environ. Sci. Eng.* **2021**, *16*, 29. [[CrossRef](#)]
27. Ribet, S.M.; Shindel, B.; dos Reis, R.; Nandwana, V.; Dravid, V.P. Phosphate Elimination and Recovery Lightweight (PEARL) Membrane: A Sustainable Environmental Remediation Approach. *Proc. Natl. Acad. Sci. USA* **2021**, *118*, e2102583118. [[CrossRef](#)] [[PubMed](#)]
28. Zhou, Y.; Wang, Y.; Dong, S.; Hao, H.; Li, J.; Liu, C.; Li, X.; Tong, Y. Phosphate Removal by a $La(OH)_3$ Loaded Magnetic MAPTAC-Based Cationic Hydrogel: Enhanced Surface Charge Density and Donnan Membrane Effect. *J. Environ. Sci.* **2022**, *113*, 26–39. [[CrossRef](#)] [[PubMed](#)]
29. Zheng, X.; Sun, W.; Wei, N.; Bian, T.; Zhang, Y.; Li, L.; Zhang, Y.; Li, Z.; Ou, H. Bionic-Inspired $La-Zn(4,4'-Dipy)(OAc)_2$ /Bacterial Cellulose Composite Membrane for Efficient Separation of Nitrogen and Phosphorus in Water. *Mater. Chem. Phys.* **2021**, *274*, 125162. [[CrossRef](#)]
30. Song, Y.; Song, X.; Sun, Q.; Wang, S.; Jiao, T.; Peng, Q.; Zhang, Q. Efficient and Sustainable Phosphate Removal from Water by Small-Sized $Al(OH)_3$ Nanocrystals Confined in Discarded Artemia Cyst-Shell: Ultrahigh Sorption Capacity and Rapid Sequestration. *Sci. Total Environ.* **2022**, *803*, 150087. [[CrossRef](#)]
31. Fang, L.; Wu, B.; Chan, J.K.M.; Lo, I.M.C. Lanthanum Oxide Nanorods for Enhanced Phosphate Removal from Sewage: A Response Surface Methodology Study. *Chemosphere* **2018**, *192*, 209–216. [[CrossRef](#)]
32. *Total Phosphorous Measurement*; National Regulation of People's Republic of China, GB 11893-89; Ministry of Ecology and Environment of the People's Republic of China: Beijing, China, 1990.
33. Smolders, A.J.P.; Lucassen, E.C.H.E.T.; Bobbink, R.; Roelofs, J.G.M.; Lamers, L.P.M. How Nitrate Leaching from Agricultural Lands Provokes Phosphate Eutrophication in Groundwater Fed Wetlands: The Sulphur Bridge. *Biogeochemistry* **2010**, *98*, 1–7. [[CrossRef](#)]